

The orbital magnetization of single and double quantum dots in a tight binding model

A. A. Ilea¹, V. Moldoveanu¹, M. N. Ită¹, A. M. Anolescu^{1,2}, V. Gudmundsson², B. Tanatar³

¹ National Institute of Materials Physics, P.O. Box MG 7, Bucharest-Magurele, Romania

² Science Institute, University of Iceland, Dunhaga 3, IS-107 Reykjavik, Iceland

³ Department of Physics, Bilkent University, 06533 Ankara, Turkey

Abstract

We calculate the orbital magnetization of single and double quantum dots coupled both by Coulomb interaction and by electron tunneling. The electronic states of the quantum dots are calculated in a tight-binding model and the magnetization is discussed in relation to the energy spectrum and to the edge and bulk states. We identify effects of chirality of the electronic orbits and of the anti-crossing of the energy levels when the magnetic field is varied. We also consider the effects of detuning the energy spectra of the quantum dots by an external gate potential. We compare our results with the recent experiments of Osterkamp et al. [Phys. Rev. Lett. 80, 4951 (1998)].

73.21.-b, 73.23.Ra, 75.75.+a

I. INTRODUCTION

The magnetic properties of mesoscopic systems are of recent experimental and theoretical interest because they give insight on the electronic structure of the system in a noninvasive way, in contrast to the transport studies¹ which are strongly dependent on the contacts necessary to measure the electric current and the voltage. Also, while the transport properties of the quantum dots depend on the processes that occur at the Fermi level, the magnetic properties are determined by the whole energy spectrum of the mesoscopic system. The origin of the orbital magnetism consists in the permanent currents carried by the quantum eigenstates in the presence of the magnetic field and of the confinement. The currents are related to the energy spectra of the system under consideration. For instance, the chirality of the current carried by one electron, which gives the direction of the corresponding magnetic moment, can be deduced from the dependence of the corresponding eigenenergy on the magnetic field. In general, the spectral properties of the system determine the sample-dependent characteristics of the magnetization.

The study of orbital magnetism under mesoscopic conditions was initiated theoretically,^{2,3} especially for predicting the role of the boundaries of the samples. An enhancement of the magnetization as compared to the Landau diamagnetism of two-dimensional (2D) electrons was demonstrated.³ More recently an exactly solvable model of non-interacting electrons has been used for simulating persistent currents and obtaining the orbital magnetization. This study has shown that the currents are much more sensitive to the geometry of the system than the associated magnetization.⁴ Bogachev et al.⁵ have shown, by analytical calculations, for circular and non-circular quantum dots with many (noninteracting) electrons that the oscillations of the magnetization with increasing the magnetic field have a hierarchy of three characteristic frequencies, due to the oscillations of the energy levels in the vicinity of the Fermi energy, due to the Aharonov-Bohm interference, and due to the de Haas-van Alphen (dHvA) effect, respectively. The importance of the electron-electron interaction in quantum dots being generally admitted, the consequences for the magnetization of 2D electron systems have been studied for finite and infinite modulated systems,⁶ and also for noncircular dots.^{6,7} In the quantum Hall regime, an enhancement due to exchange and correlation was shown both experimentally and theoretically.⁸ Other recent measurements of the dHvA oscillations, showing clear sawtooth profiles, have been performed by Wiegers et al.⁹ and by Harris et al.¹⁰ For quantum dots, an ingenious indirect technique was used by Osterkamp et al.,¹¹ in order to evaluate the change in the magnetization due to single electron tunneling, from transport measurements. Only very recently the magnetization of arrays of quantum dots have been directly measured, but insufficiently understood.¹²

Since the magnetic moment of an individual dot is extremely small, the experimental endeavor is oriented nowadays towards the study of bigger ensembles in order to measure a cumulative effect. In this case, the dots can be coupled to each other either only electrostatically, or also exchanging electrons by tunneling, so that, in principle, the magnetization of the ensemble of coupled dots may be very different from the scaled magnetization of an individual dot. In order to be able to distinguish between these two situations, one has to know beforehand the behavior of one single dot and then to identify the coupling effects.

The aim of this paper is a parallel study of magnetic properties of single and double

dots in the presence of the electrostatic coupling, resonant tunneling, and detuning. The double dot is viewed as a coherent quantum-mechanical system separated in two regions by a constriction that can be controlled by a parameter. The intra- and inter-dot electron-electron interaction is taken into account on the same footing, and the detuning between the two regions is realized by applying an external potential (or bias) on only one of them. The modifications in the energy spectrum, topology of local currents and the consequences for the orbital magnetization will be presented.

II. THE TIGHT-BINDING MODEL AND ITS RANGE OF VALIDITY

We describe the 2D electron system in perpendicular magnetic field by a discrete, tight binding (TB) Hamiltonian, defined on a rectangular lattice (or plaquette). The lattice consists of N sites along the x - and M sites along the y -direction, separated by an inter-site distance a , so that a lattice vector reads $\mathbf{r}_{nm} = na\mathbf{e}_x + m a\mathbf{e}_y$, with n, m integers. Choosing the symmetric gauge for the vector potential, the one-electron spinless Hamiltonian reads:

$$H = \sum_{n,m} \langle \mathbf{r}_{nm} | H | \mathbf{r}_{nm} \rangle + t \sum_{n,m} e^{i\mathbf{A}(\mathbf{r}_{nm})} \langle \mathbf{r}_{nm} | H | \mathbf{r}_{n+1,m} \rangle + t \sum_{n,m} e^{i\mathbf{A}(\mathbf{r}_{nm})} \langle \mathbf{r}_{nm} | H | \mathbf{r}_{n,m+1} \rangle + \text{h.c.} \quad (2.1)$$

In this expression, $|\mathbf{r}_{nm}\rangle$ is a set of orthonormal states localized at the sites \mathbf{r}_{nm} and \mathbf{A} is the magnetic flux through the unit cell measured in quantum flux units, $\Phi = B a^2 / \Phi_0$; $\Phi_0 = 1.43 \cdot 10^{-15}$ Weber. The hopping energy $t = \hbar^2 / 2m a^2$ will be considered as the energy unit and the lattice constant a will be the length unit. The choice of the boundary conditions is essential for the spectral properties of the Hamiltonian (2.1) and the orbital magnetism. The cyclic boundaries give rise to the Hofstadter butterfly if the commensurability of the geometric and magnetic periods is ensured.¹³ For the finite system the natural boundary conditions are of Dirichlet type, in which case the commensurability condition is not necessary, and a quasi-Hofstadter spectrum, with edge states filling the gaps, is obtained. Also the degeneracies specific to the usual Hofstadter spectrum (at $B \neq 0$) are lifted by the presence of the infinite walls.^{14;15}

Our discrete system can be easily tailored into various shapes, or into several subsystems, by removing some inter-site hopping terms, or by imposing infinite barriers at some sites. For instance, we can model one single quantum dot, and two or more coupled dots. One question is whether a real system can be reasonably described by such a discrete model. The interatomic distance for GaAs is $a \approx 0.35$ nm which means that if we wish to reach the atomic resolution for a square dot of linear dimensions $L = 100$ nm, we need a lattice of 1000×1000 sites. Obviously this requires too much memory and computing power, and we must restrict to a smaller number of sites. In reality we need much less sites. For instance, a grid containing 20×20 sites corresponds to an inter-site distance $a \approx 5$ nm. In addition we have to specify the strength of the magnetic field and the number of electrons. Obviously, the magnetic length $l_B = (\hbar / eB)^{1/2}$ must be larger than the inter-site distance a , or equivalently

$$B < 1/2 \quad (2.2)$$

Therefore, to describe the square dot of 100 nm \times 100 nm by a lattice of 20×20 sites, we have to consider $B < 20$ T, which actually covers a wide range of experimental interest. As another example, a grid 10×10 satisfies the same condition only for smaller fields $B < 5$ T.

Since the energy spectrum of the one-band 2D tight-binding model contains $N - M$ (nondegenerate) eigenvalues, and is bounded in the interval $[-4t; 4t]$, it can accommodate at most $N - M$ spinless electrons. Thus, the condition (2.2) must be supplemented by the requirement $k_{F \text{ermi}} < 1/a$ which ensures that the cosine-type tight-binding spectrum approximates well the parabola of the quasi-free electrons at low magnetic fields. In terms of energies the condition can be written as

$$E_{F \text{ermi}} < 2t; \quad (2.3)$$

the Fermi energy being measured from the bottom of the spectrum. Evidently, a finer grid means a denser spectrum and a larger number of electrons. The second condition indicates that a 20×20 plaquette provides a reasonable approximation for a system of about 100 electrons. In general we shall keep the number of electrons N_e below $N - M = 3$. Altogether, the above conditions show that the lattice model describes correctly a physical quantum dot if the electrons occupy only the states corresponding to the bottom-left corner of the quasi-Hofstadter spectrum.

Several papers used the tight-binding model to describe single quantum dots as we do here,^{16,17} or groups of coupled quantum dots.^{18,19} (In the later case each dot was associated to a single site of the lattice and had therefore no internal structure.) The alternative to the discrete model is to consider a quantum dot defined by a continuous confining potential, to expand the one-electron wave functions in a set of basis functions and to diagonalize the corresponding Hamiltonian matrix. But for the numerical calculations the basis has to be truncated to a finite set, which is in fact equivalent to choosing a finite number of sites in the tight-binding model. The bigger the basis, the bigger the number of electrons ordered in the dot. The natural basis functions are the Laguerre polynomials, and for reasonable results one needs at least 2-4 times more basis functions than electrons. On the other hand, the computational effort increases exponentially with the size of basis set, such that for a non-circular and non-parabolic dot one can hardly go beyond 4-6 electrons.⁷ Instead, in the tight-binding model we can consider 50-100 electrons or more, for any shape of the dot.

III. MAGNETIZATION OF A SINGLE DOT

In this section we discuss the relation of our tight-binding Hamiltonian (2.1) and the orbital magnetization of the system. The one-body Hamiltonian can be formally written as

$$H = \sum_{nm} \sum_{\alpha\beta} H_{nm, \alpha\beta} |j\alpha\rangle \langle j\beta|; \quad (3.1)$$

where $H_{nm, \alpha\beta} = \langle j\alpha | H | j\beta \rangle$ are the matrix elements of H . We denote its eigenvalues by E and its eigenstates by $|j\rangle$. The position operator for an electron on the lattice can also be written as

$$r = \sum_{nm} r_{nm} |j\rangle \langle j|; \quad (3.2)$$

and obviously r_{nm} and $|j\rangle$ are eigenvalues and eigenvectors of the position operator. Then, the operator associated with the current carried by one electron of charge $e > 0$ is

$$\underline{J} = -\frac{ie}{h} [\underline{H}; \underline{r}] = -\frac{ie}{h} \sum_{nm, n'm'} H_{nm, n'm'}(\underline{r}_{nm} - \underline{r}_{n'm'}) \hat{j}_{nm}^0 \hat{j}_{n'm'}^0; \quad (3.3)$$

and obviously any eigenstate of \underline{H} has a zero average current, $\langle \underline{j} \rangle = 0$. The terms of the sum in Eq. (3.3) can be interpreted as the currents from the site nm to the site $n'm'$,

$$J_{nm, n'm'} = \frac{ie}{h} [H_{nm, n'm'}(\underline{r}_{nm} - \underline{r}_{n'm'}) \hat{j}_{nm}^0 \hat{j}_{n'm'}^0 + H_{n'm', nm}(\underline{r}_{n'm'} - \underline{r}_{nm}) \hat{j}_{n'm'}^0 \hat{j}_{nm}^0] : \quad (3.4)$$

With Eq. (3.4) we can calculate the distribution of the current within the system, while Eq. (3.3) is sufficient to define the magnetization operator for one electron, as the standard orbital magnetic moment,

$$\underline{M} = \frac{1}{2} \underline{r} \times \underline{J} = \frac{1}{2} (xJ_y - yJ_x) \underline{e}_z : \quad (3.5)$$

For a given eigenstate of the Hamiltonian the average magnetization is obtained, by combining Eqs. (3.2) and (3.3), as

$$\langle \underline{M} \rangle = \frac{2e}{h} \sum_{nm, n'm'} \langle \text{Im} [H_{nm, n'm'} \langle \hat{j}_{nm}^0 \hat{j}_{n'm'}^0 \rangle] \rangle : \quad (3.6)$$

This result does not depend on the way the sites are coupled (nearest neighbors, next-nearest neighbors, etc.), nor on the presence of the Coulomb interaction. It holds as long as we use a one-body Hamiltonian. In particular, in the Hartree approximation, the interaction changes the states $|j\rangle$, but not the current operator Eq. (3.3), which is insensitive to the diagonal matrix elements of the Hamiltonian. (However, in the Hartree-Fock approximation the interaction becomes visible also in the current operator.)

At fixed magnetic field, the ground state magnetization M_g is calculated by summing up the individual contributions M of all occupied eigenstates:

$$M_g(B) = \sum_{E \leq E_F} M : \quad (3.7)$$

In the localized representation the current density $\underline{j}(\underline{r})$ reads:

$$\underline{j}(\underline{r}) = \frac{ie}{h} \sum_{nm} (\underline{r} - \underline{r}_{nm}) \sum_{n'm'} H_{nm, n'm'}(\underline{r} - \underline{r}_{n'm'}) \hat{j}_{nm}^0 \hat{j}_{n'm'}^0 + \text{h.c.} : \quad (3.8)$$

The TB model provides a quick proof of the fact that \underline{M} defined above coincides with $\langle \underline{j} | d\underline{H} = d\underline{B} | \underline{j} \rangle$, and thus, from the Feynman-Hellman theorem, with $dE = d$. Indeed, from (2.1):

$$\frac{dH}{dB} = \frac{a^2}{0} \frac{dH}{d} = \frac{i}{0} \frac{a^2 \tau}{nm} [m e^{i m} \hat{j}_{nm}^0 \hat{j}_{nm+1}^0 + n e^{i n} \hat{j}_{nm}^0 \hat{j}_{nm+1}^0] + \text{h.c.} : \quad (3.9)$$

which gives immediately Eq. (3.6). The same result can be obtained by defining the magnetization as the the magnetic moment density ($\mu_B = 2m_e \hbar$) $\underline{j}(\underline{r})$ integrated over the whole area.²⁰

The sign of M is determined by the chirality of the corresponding eigenstate, that is by the sign of the derivative $dE_n/d\phi$, which can be easily observed from the quasi-Hofstadter spectrum. The edge and bulk states coexist at strong magnetic fields, have opposite chiralities, so that their contributions to the total magnetic moment have different signs, and eventually may cancel each other. An example is given in Fig.1 which shows the magnetization carried by the first 120 eigenstates of a 20×20 plaquette at $\phi = 0.1$, corresponding to a square quantum dot of width about 100 nm, at $B = 15$ T.

Since the bulk and the edge states generate intercalated bands and quasi-gaps in the spectrum, one may guess an oscillatory behavior of the total magnetization M_g of the quantum dot as a function of the number of electrons accommodated inside. For an infinite system these oscillations become the well known sawtooth profile of the total magnetization, the dHvA oscillations in the regime of strong magnetic fields. Recent experiments have shown them for extended, theoretically infinite samples,^{9,8} but, to our knowledge, nothing has been reported yet for finite samples, i.e. when the contribution from the boundaries of the system is expected to be important, except theoretical results.^{5,6,21}

In the low field regime the situation is changed: the spectrum of our system is no longer organized into bands and gaps, and the consecutive states may have alternating chiralities. Therefore the summations of all contributions must give rise to much faster, eventually chaotic oscillations of the magnetization as a function of the number of electrons. This case was studied by Shapiro, Hajdu and Gurevich³ by calculating the magnetic susceptibility in the grand-canonical ensemble. Their result – for square geometry – is a rapidly oscillating comb-type picture which demonstrates an enhancement compared to the Landau susceptibility.³ Here we calculate M_g as a function of N_e at $\phi = 0.001$ ($B = 0.15$ T) and obtain also a comb-like picture which is shown in Fig.2.

From an experimental point of view, it is more interesting to analyze the magnetization as a function of the magnetic field B . With increasing B , but for a constant number of electrons, the magnetization also oscillates changing the sign when the Fermi level crosses regions of different chiralities. The internal mechanism can be understood from Figs. 3(a)–(b) which show the quasi-Hofstadter spectrum and the magnetization of a 10×10 plaquette occupied by 10 electrons. One notices that the spectrum contains numerous anti-crossing points where the slope of the energy levels change suddenly, together with the chirality of the corresponding current. In fact, at these transitions the states change from edge to bulk states, or vice versa. However, for the total magnetization only the anti-crossings at the Fermi level are important. The change of sign of the magnetic moment of that state changes abruptly the total magnetization. Instead, the anti-crossings below E_F do not change the total magnetization because there is always a compensation between two adjacent levels. Indeed no compensation occurs at the Fermi level.

For a large number of electrons, the Fermi level increases to a region with a huge number of anti-crossings, yielding fine and super fine oscillations of the magnetization obtained by Bogachev et al. for dots with 2500 electrons.⁵ We approach this regime in Figs. 4(c)–(d), for 100 electrons on a 20×20 plaquette. The big oscillations of the magnetization are precursors of the dHvA effect occurring at strong magnetic fields, while the small oscillations reflect the anticrossing points in the energy spectrum at the Fermi energy.

Some disorder, if present in the system, would lift the degeneracies but would also smoothen the anti-crossing regions. Consequently, the oscillations of the magnetization

would become also smoother than shown in our Fig.3, and indeed, the same would happen at a finite temperature. We shall see in the next section that the electron-electron interactions have a similar effect.

The analysis of the magnetization based on the spectral properties is done here for a square geometry and a tight-binding model. The results obtained in Ref.⁷ prove however that the conclusions are model independent. In that paper, a similar behavior showing smooth regions and jumps of the magnetization as a function of the field have been found for circular and elliptic dots with 2-5 electrons, in the continuum model based on the Darwin-Fock Hamiltonian. It was shown that the positions of the jumps in magnetization can be identified also from the maxima of the total energy as a function of magnetic field.

As function of $l=B$, the dHvA oscillations are almost equidistant, with amplitude and period depending on the number of electrons N_e , as shown in Fig. 4 (a). In the scaled variables M_g/N_e and N_e/B we find that all the curves coincide rather well, which is shown in Fig. 4 (c). From this scaling property one concludes that the period of the dHvA oscillations is $(l=B) = \text{const} = N_e$. This result differs from the usual problem of dHvA effect in metals where the period is proportional to $l=E_F$, while E_F is considered in good approximation independent of B . It turns out that for small confined systems this is not true, the Fermi energy exhibiting large oscillations with maxima coinciding with the peaks of the magnetization, as illustrated in Fig. 4 (b).

The scaling of the magnetization curves suggests that the magnetization per particle of a quantum dot can be written as

$$\frac{M_g}{N_e} = f \left(\frac{N_e}{B} \right); \quad (3.10)$$

where $f(x)$ is an oscillating function in the high field regime and it is nearly constant at low fields.

In principle the spin may play an important role in the magnetization. However, in the present paper we neglect the spin.^{5,22} The orbital magnetization in GaAs is enhanced due to the effective mass by 14.9, compared to the spin contribution. The spin magnetization is in general small at moderate or low magnetic fields, when the Zeeman energy is much smaller than the cyclotron energy. In a first approximation the spin contribution is independent on the current distribution and consists in relatively weak oscillations around zero, see e.g. Fig. 6 of Ref.⁶

As mentioned in the Introduction we intended to identify possible effects produced by the tunneling and electrostatic coupling between the dots. Such effects are important because the magnetization is measurable only for ensembles, and not for individual dots.¹² Both types of coupling have a considerable influence on the orbital part of the wave functions, and consequently on the orbital magnetization. This justifies more attention to the orbital magnetization for multi-dot systems.

IV. DOUBLE DOTS: TUNNELING AND ELECTROSTATIC EFFECTS

We consider now two coupled quantum dots, and label them 1 and 2. The inter-dot tunneling, electron-electron interaction, and detuning introduce specific aspects in the distribution of charge and persistent currents which affects the orbital magnetization. The

double dot is sketched in Fig.5, and it is considered as a unique coherent quantum system described by the Hamiltonian

$$H = H_1(\mathbf{r}) + H_2(\mathbf{r}; V_g) + H_{12} + H_{el-el}; \quad (4.1)$$

where H_1 and H_2 correspond to the individual dots and are the same as in Eq. (2.1). The two dots are coupled both by the tunneling term H_{12} , and by the electron-electron interaction H_{el-el} which here is considered in the Hartree approximation. In addition we also consider a gate potential V_g applied on the second dot, i.e. a detuning parameter, which yields an energy offset between the two subsystems, and consists of an extra diagonal term in H_2 .

The inter-dot resonant-tunneling term is

$$H_{12} = \sum_{n_1 m_1, n_2 m_2} c_{n_1 m_1, n_2 m_2} \hat{n}_{1 m_1} \hat{n}_{2 m_2} + h.c.; \quad (4.2)$$

where the sites $(n_1 m_1)$ and $(n_2 m_2)$ belong to the first, and to the second dot, respectively. The sites $(n_1 m_1)$ and $(n_2 m_2)$ are connected or not if $c_{n_1 m_1, n_2 m_2} = 1$ or 0.

For the Coulomb interaction we use the Hartree approximation. The exchange interaction might be important at high magnetic fields (even if the spin is ignored), usually well above 1 Tesla.^{6,8} As we have checked, in the Hartree-Fock approximation the exchange effects are not important for the tight-binding model, in the regime studied in this paper. In a recent paper Creeld et al. have studied a continuous square quantum dot with two electrons in a weak magnetic field by exact diagonalization, and found a good agreement with the tight-binding model in the Hartree approximation.²²

The Coulomb interaction, in the Hartree approximation, reads

$$H_{el-el} = U_c \sum_{n m} \sum_{n' m'} \frac{N_{n' m'}}{(\mathbf{r}_{n m} - \mathbf{r}_{n' m'})^2 + (\mathbf{r}_{n m} - \mathbf{r}_{m' 0})^2} \hat{n}_{n m} \hat{n}_{n' m'}; \quad (4.3)$$

where $N_{n m}$ is the mean occupation number of the site $\mathbf{r}_{n m}$ and has to be calculated self-consistently with the energy levels. The Coulomb energy, in units of t , becomes $U_c = e^2/\epsilon$ at $\epsilon = 1$ where we have used the dielectric constant $\epsilon = 12.4$ and the effective mass $m_e = 0.067$ as for GaAs. However, for $U_c = 1$ it is technically difficult to obtain the convergence of our iterative numerical scheme. Therefore, being in fact interested in qualitative results, we use in our calculation a lower value, $U_c = 0.4$, which still produces a strong perturbation of the noninteracting states. If we assume the physical dimension of each quantum dot to be 50 nm, and we choose a rectangular plaquette of 10×20 sites to model the double-dot system, meaning a 5 nm , our U_c corresponds to a Coulomb energy of about 8 meV.

We first consider no exchange of electrons between the dots, i.e. $\epsilon = 0$, and we focus our attention on the effects induced by the electron-electron interaction. In principle, this interaction may play a role in the magnetic properties of the dots since it produces rearrangements of the electric charge and of persistent currents. One may distinguish between intra-dot and the inter-dot interaction, the latter being the electrostatic coupling between dots. We would like to find out which one is more important from the point of view of the orbital magnetism.

It has already been observed that in confined systems the bulk states are more sensitive to the Coulomb interaction than the edge states.^{6,23} By calculating the Hartree spectrum, for

a fixed number of electrons, we find that the energy distance between the bulk-type states, which almost form energy 'bands', increases, while the energy of the edge states remains almost fixed. Therefore the Coulomb interaction mixes the energies of bulk-type and edge-type states, and thus states with opposite chirality become intercalated also in the 'bands'. This can be seen in Fig.6, even in the absence of the inter-dot interaction. A supplementary repulsion is added when the inter-dot interaction is taken into account, and further changes occur in the spectrum. One also notices that the electron interaction contributes to the repulsion of the levels at the anti-crossing points.

The magnetic moments M of the Hartree states are sensitive to these effects and incorporate both the broadening of the bands and intercalation of states with opposite chirality. We intend to find out the role played by the electron-electron interaction, in general, and by the inter-dot coupling, in particular. Comparing the two curves of M_g versus B in Fig.6, we observe that the inter-dot coupling attenuates the jumps and rounds off the peaks. This happens mainly at low fields. The comparison of the magnetization shown in Fig.3, where $U_c = 0$, and those shown in Fig.6 indicate that the major interaction effect in the magnetization comes from the inter-dot coupling. Also, for intermediate and high magnetic fields, the saw-tooth shifts slightly, as was already noticed in Ref.⁷ However, the magnetic susceptibility $\chi = dM/dB|_{B=0}$ is not affected by the presence of the electrostatic coupling. We shall see below that this is not the case in the presence of tunnel coupling.

We now consider the role of the tunneling, which means $t \neq 0$. To be within the tunneling regime, we choose $t = 0.4t$. The tunneling now lifts the two-fold degeneracy of the eigenstates of the double dot, and doublets of states appear now in the spectrum. On the other hand, the eigenfunctions and the associated persistent currents penetrate the constriction and are distributed spatially over the whole area of the double dot. Under these circumstances, the distinction between edge- and bulk-states, which is applicable for single dots, becomes improper. Mixed states may also occur as shown in Fig.7 (middle panel).

This means that the chirality of a state can no longer be guessed from the localization of that state in the bulk or at the edge of the sample. In the absence of the interaction the current associated with the lowest-energy eigenstate of the double dot is distributed in the middle of each dot, as shown in Fig.7 (top panel). But the Coulomb repulsion pushes the current distribution towards the edges, as shown in Fig.7 (bottom panel). In the mixed state # 46 the current shows, in different regions, either clockwise or anti-clockwise circulation so that the total chirality of the state can only be found by the explicit calculation of the corresponding magnetization M_{46} .

The numerical calculation of the total orbital magnetization, shown in Fig.8, indicates that its dependence on the magnetic field is affected by the resonant coupling only in the low-field domain where the sharp peaks are again smeared (for 10 electrons per dot this occurs below $B = 2T$). Unlike the case of electrostatic coupling, the resonant tunneling modifies the magnetic susceptibility. Indeed, for the situation presented in Fig.8, the slope at $B = 0$ remains negative but is smaller in magnitude compared to the $t = 0$ case.

V. REDISTRIBUTION OF CHARGE IN DETUNED DOUBLE DOTS

When one of the dots has a different confinement than the other, or is subjected to a supplementary gate potential V_g , its individual energy spectrum is detuned with respect to

the spectrum of the other dot. For the sake of definiteness we consider a negative gate potential, such that the dot 2 in Fig.5 gains positive electrostatic energy, $eV_g > 0$, being pushed energetically upwards. We assume each dot is of linear dimension $L = 100 \text{ nm}$, and is described by a 10×10 lattice.

The role of the detuning was emphasized in connection with the transport properties of double quantum dots.²⁴ The differences in the energy levels of the two dots can block the transfer of electrons. The absence of the resonance condition implies the absence of doublets in the spectrum (case discussed in the previous section) and also a strong divergence of permanent currents at the constriction between dots.

By varying continuously V_g , one allows the redistribution of the electrons between the two dots. Even for a weak inter-dot tunneling (i. e. $\epsilon \neq 0$, but small), the magnetization behaves in an interesting fashion. In order to understand the physical process, let us consider the case of nearly isolated dots. The spectra of the two dots are identical, but shifted by eV_g . Then by changing the gate potential, a series of resonances occur and at each resonance, one electron is transferred from the dot 2 to the dot 1. The transfer may be accompanied by a change of chirality if, for instance, the electron moves from an edge state to a bulk state. Then, at the corresponding value of the gate potential, the orbital magnetization of the whole system has a jump, together with the occupation numbers of each individual dot. The jump of magnetization can be positive or negative, depending on the chiralities of the initial and final states. Both situations are visible in the top panel of Fig.9.

At a fixed magnetic field, the energy spectrum of the double dot contains a multitude of anti-crossing points between the levels of the dot 1, the horizontal lines in the bottom panel of Fig.9, and of the detuned dot 2, the lines with slope about 1. Indeed, in Fig.9 one can see that the jumps of the magnetization, and of the numbers of electrons in each dot, occur simultaneously with the condition $E_N = E_{N+1}$, E_N being the highest occupied level of the double dot. The redistribution of the electrons means that the system undergoes a transition from the configuration $(N_1; N_2)$ to $(N_1 + 1; N_2 - 1)$, where N_1 and N_2 are the numbers of electrons in the first and the second dot respectively, and $N_1 + N_2 = N$ is the total number of electrons in the system. Then, the jump of the ground state magnetization can be expressed in terms of the magnetic moments carried by the eigenstates of the dots:

$$M_g = M_g(N_1; N_2) - M_g(N_1 + 1; N_2 - 1) = M_{N_1+1}^{(1)} - M_{N_2}^{(2)}; \quad (5.1)$$

where $M_{N_1+1}^{(1)}$ and $M_{N_2}^{(2)}$ are the magnetic moments carried by the states $|N_1 + 1\rangle$ and $|N_2\rangle$, in the dots 1 and 2, respectively.

This situation actually occurs only for weak inter-dot coupling. Obviously, a stronger coupling spoils the quantization of the number of electrons and of the magnetization, that is the steps are less sharp and the plateaus less evident, as shown by the dashed lines in Fig.9.

As a function of the magnetic field, the spectrum of a double dot develops a dual aspect obtained by the mixing of the two Hofstadter spectra of individual dots with a relative shift of eV_g . For instance, some eigenvalues originating in the first quasi-gap of one dot overlap with the second band corresponding to the spectrum of the second dot. A similar situation occurs also for higher energies. The effect of the mixing on the total magnetization is shown in Fig.10 (b) where many secondary peaks can be noticed as compared to Fig.3. The differences are thus produced by the numerous anti-crossing points in the spectrum of the double dot which appear at the intersection of the two detuned quasi-Hofstadter spectra.

In closing this section we mention that by including the Coulomb interaction we obtained similar results, without important qualitative differences.

VI. CONCLUSIONS

Our general aim was to demonstrate the correlation between the spectral properties and the orbital magnetization of a quantum dot, by considering that the orbital magnetization is the sum of the individual orbital magnetic moments of all eigenstates. The electrostatic and tunneling coupling of two quantum dots also bring new effects. We have noticed that the anti-crossing points in the spectrum have special significance because of the sudden change in the chirality of the electronic orbits occurring at these points, with corresponding sign changes of the magnetic moments.

We have shown that interesting conclusions can be deduced even only from the field dependence of the Fermi energy. This is because the anti-crossing effect at the Fermi level cannot be compensated by the opposite contribution of the adjacent level, which is empty. So, we have put forward the argument for which the tunneling transport data can be relevant for the magnetic properties. Osterkamp et al.¹¹ took advantage of this fact and performed an indirect measurement of the changes in the magnetization under resonant conditions in double dots. In the experiment, by sweeping the gate voltage V_g at different magnetic fields B , one identifies all pair values $(V_g; B)$ when a peak in the tunneling current occurs. Then, a change in magnetization should occur, as we have discussed in the previous section. In Ref.¹¹ the change ΔM is calculated as being proportional to $\Delta V_g = B$. The sign of ΔM can be positive or negative as we have also found in Fig. 9 (a). We have stated also that the sign is determined by the relative chiralities of initial and final states.

The experiments¹¹ were done in the weak coupling limit when the mixing of the two spectra is negligible and, intuitively, one may think in terms of alignment of energy levels. In our approach, this condition is not compulsory since the double dot is treated as a coherent quantum system. In the case of a larger coupling the anti-crossings, the depletion of the detuned dot and the changes in magnetization become more smooth.

The electron-electron interaction, mainly the inter-dot component, affects the distribution of the persistent currents and attenuates the oscillations of the orbital magnetization especially at low fields. Nevertheless, according to our results the magnetic susceptibility is not influenced by the electrostatic coupling. A scaling behavior of the quantum dot magnetization as a function of magnetic field at different number of electrons has been identified in the dHvA regime.

ACKNOWLEDGMENTS

M.N. and V.M. were supported by NATO-PC TUBITAK Programme, and B.T. by TUBITAK, TUBA, NATO-SfP, and KOBRA-001, at Bilkent University, Ankara. The research was also financed by the CNCSIS and National Research Programme, Romania, and by the Icelandic Natural Science Foundation, and the University of Iceland Research Fund.

REFERENCES

- ¹ For a recent review see, L. P. Kouwenhoven, D. G. Austing, and S. Tarucha, *Rep. Prog. Phys.* **64**, 701 (2001).
- ² J. M. Vanuitenbeek, *Z. Phys. D* **19**, 247 (1991); S. Oh, A. Yu. Zyuzin, and R. A. Serota, *Phys. Rev. B* **44**, 8858 (1991).
- ³ J. Hajdu and B. Shapiro, *Europhys. Lett.* **28**, 61 (1994); E. Gurevich and B. Shapiro, *J. Phys. I* **7**, 807 (1997).
- ⁴ W. C. Tan and J. C. Inkson *Phys. Rev.* **60**, 5626 (1999).
- ⁵ E. N. Bogachev, A. G. Scherbakov, and U. Landman, *Phys. Rev. B* **63**, 115323 (2001).
- ⁶ V. Gudmundsson, S. Erlingsson, and A. Manolescu, *Phys. Rev. B*, **61**, 4835 (2000).
- ⁷ I. Magnusdottir and V. Gudmundsson, *Phys. Rev. B* **61**, 10229 (2000).
- ⁸ I. Meinel, D. Grundler, D. Heitmann, A. Manolescu, V. Gudmundsson, W. Wegscheider, and M. Bichler, *Phys. Rev. B* **64**, 121306(R) (2001).
- ⁹ S. A. Weigers, M. Specht, L. P. Levy, M. Y. Simmons, D. A. Ritchie, A. Cavanna, B. Etienne, G. Martinez, and P. Wyder, *Phys. Rev. Lett.* **79**, 3238 (1997).
- ¹⁰ J. G. E. Harris, J. Knobel, K. D. Maranowski, A. C. Gossard, N. Samarth, and D. D. Awschalom, *Phys. Rev. Lett.* **86**, 4644 (2001).
- ¹¹ T. H. Oosterkamp, S. F. Godijn, M. J. Uilenreep, Y. V. Nazarov, N. C. van der Vaart, and L. P. Kouwenhoven, *Phys. Rev. Lett.* **80**, 4951 (1998).
- ¹² M. P. Schwarz, D. Grundler, M. Wilde, C. Heyn, and D. Heitmann, *J. Appl. Phys.* **91**, 6875 (2002).
- ¹³ R. D. Hofstadter, *Phys. Rev. B* **14**, 2239 (1976).
- ¹⁴ P. Streda, J. Kucera, D. Pfannkuche, R. R. Gerhardt, and A. H. MacDonald, *Phys. Rev. B* **50**, 11955 (1994).
- ¹⁵ A. A. Iida, P. Gartner, A. Manolescu, and M. Nita, *Phys. Rev. B* **55**, 13389R (1997).
- ¹⁶ C. M. Canali, *Phys. Rev. Lett.* **84**, 3934 (2000).
- ¹⁷ R. Berkovits and U. Sivan, *Europhys. Lett.* **41**, 653 (1998).
- ¹⁸ R. Kotlyar, C. A. Stafford, and S. Das Sarma, *Phys. Rev. B* **58**, 3989 (1998).
- ¹⁹ G. Kirczenow, *Phys. Rev. B* **46**, 1439 (1992).
- ²⁰ J. Desbois, S. Ouvry, and C. Texier, *Nucl. Phys. B* **528**, 727 (1998).
- ²¹ M. Nita, A. A. Iida, and J. Zittartz, *Phys. Rev. B* **62**, 15367 (2000).
- ²² C. E. Creel, J. H. Jefferson, S. Sarkar, and D. L. J. Tipton, *Phys. Rev. B* **62**, 7249 (2000).
- ²³ V. Moldoveanu, A. A. Iida, A. Manolescu, and M. Nita, *Phys. Rev. B*, **63**, 045301 (2001).
- ²⁴ G. Klinck, G. Chen, and S. Datta, *Phys. Rev. B* **50**, 2316 (1994).

FIGURES

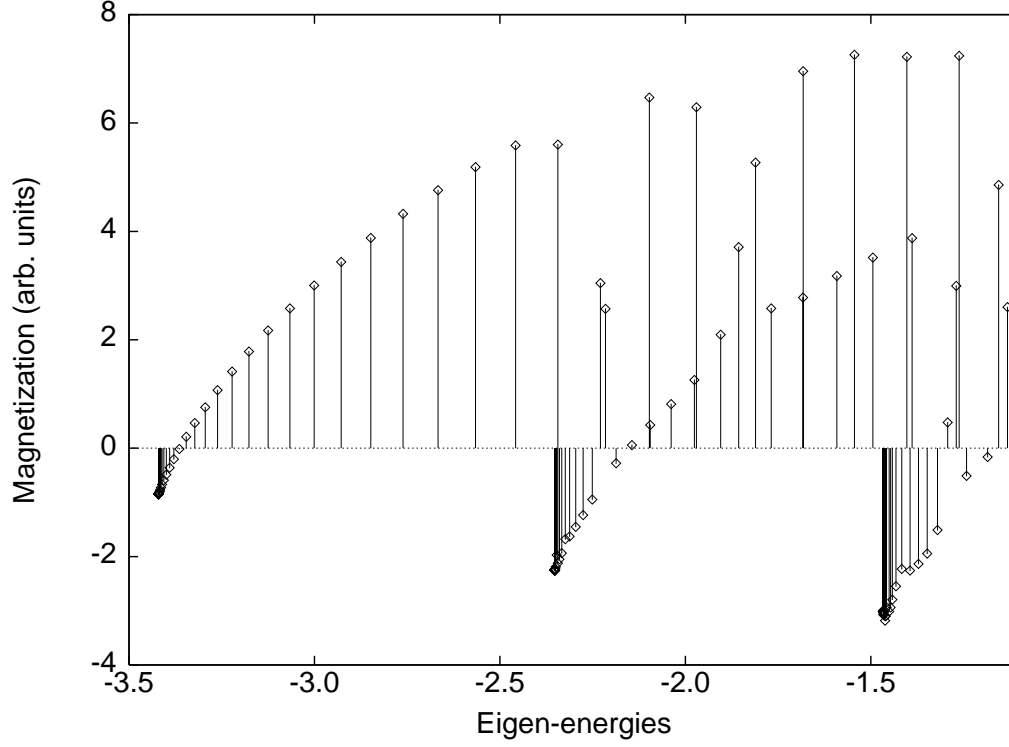


FIG .1. Magnetizations M for each of the first 120 eigenstates, for a lattice model of 20×20 sites, in the high-field regime, $\mu = 0.1$ (or $B = 15$ T, see text). The negative magnetizations grouped in bands correspond to bulk states, the positive ones fill the gaps and correspond to edge states.

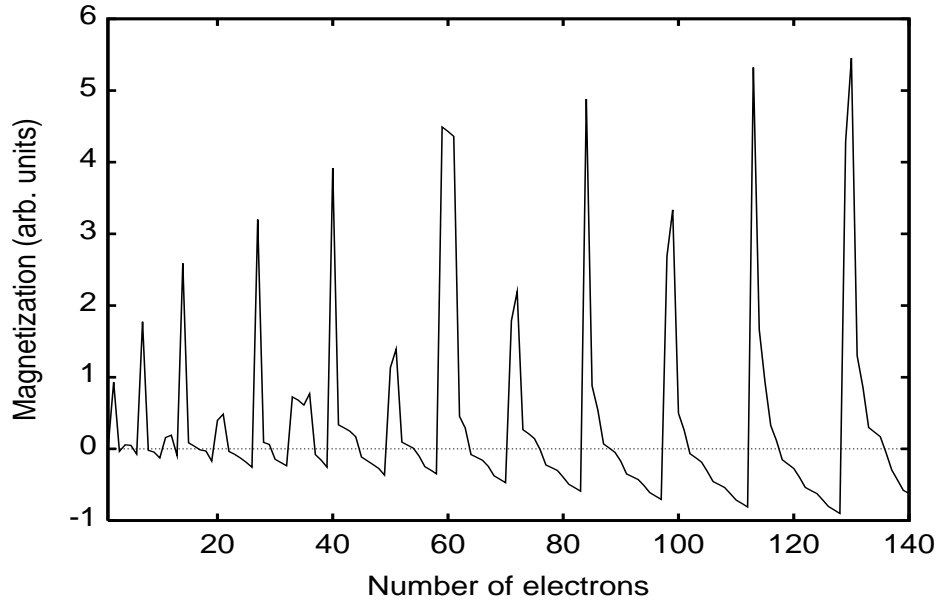


FIG. 2. Total orbital magnetization as function of the number of non-interacting electrons in the low field regime, $\mu_B = 0.0001$ (B = 0.015 T). The square dot of dimension $L = 100$ nm is represented in the tight-binding model by a plaquette of 20×20 sites.

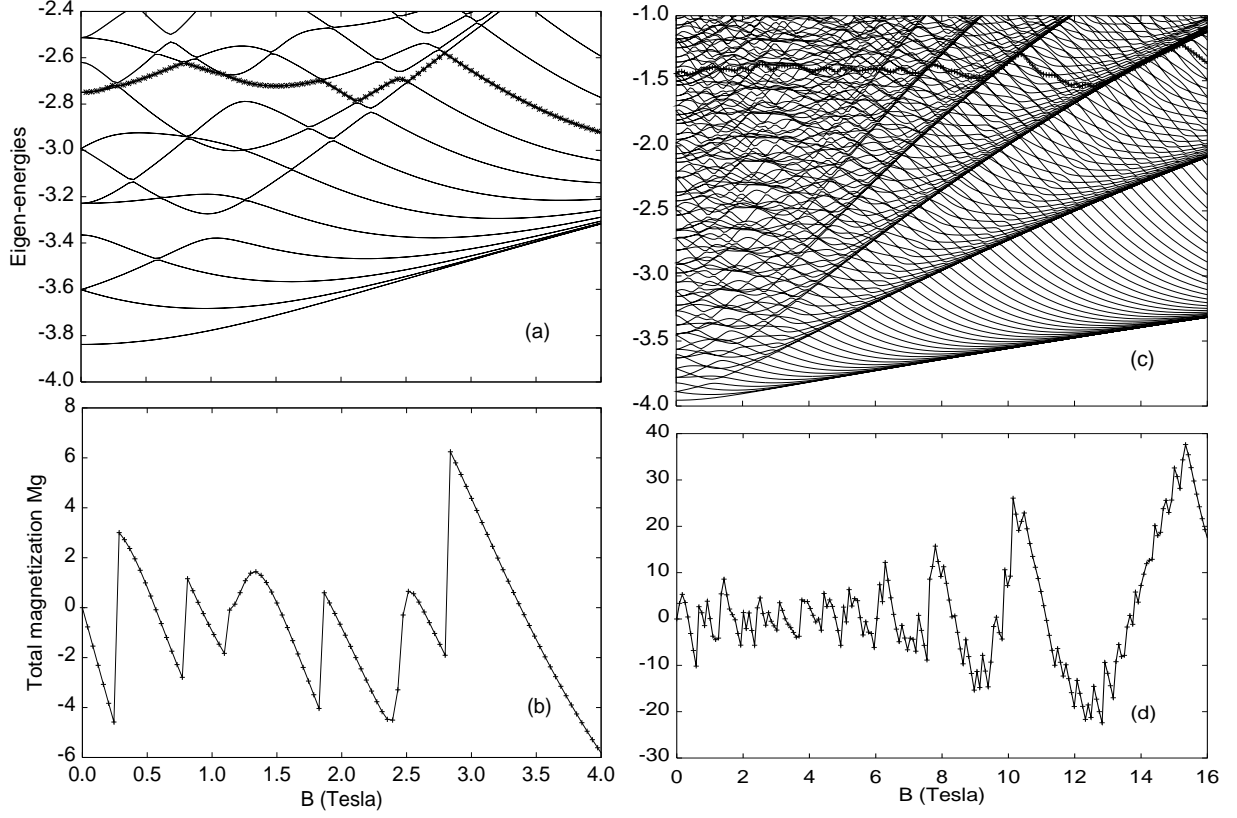


FIG .3. (a) -The dependence of the spectrum and Fermi energy (with crosses) on the magnetic field, for a square 10×10 plaquette with 10 non-interacting electrons. (b) - The corresponding total orbital magnetization. The jumps in magnetization correspond to the change of the sign of dE_F/dB . (c) - The energy spectrum for a 20×20 plaquette, with 100 non-interacting electrons, and (d) - the magnetization.

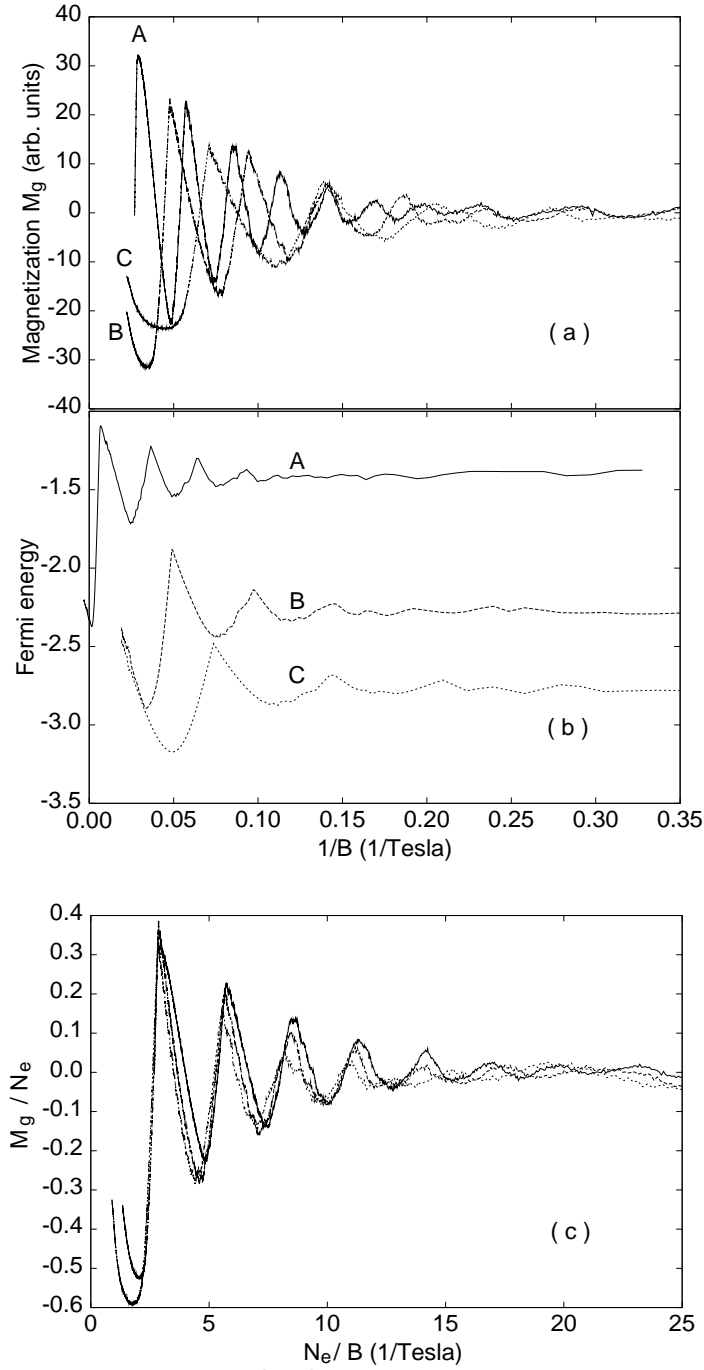


FIG .4. (a) –The magnetization of a square quantum dot $L = 100$ nm versus the inverse magnetic field for different numbers of electrons: 100 (curve A), 60 (curve B), 40 (curve C). (b) –The Fermi energy for the same numbers of electrons. (c) –The scaled representation : magnetization per particle M_g/N_e versus N_e/B ; the three curves a,b,c drops in a single one.

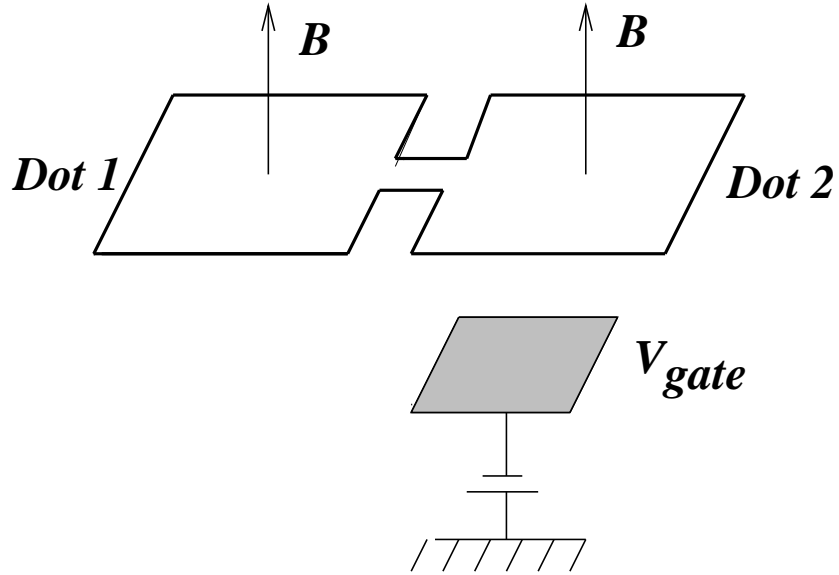


FIG . 5. Sketch of a double dot: tunneling may occur through the constriction (the central channel) and a gate voltage applied on the second dot produces detuning effects.

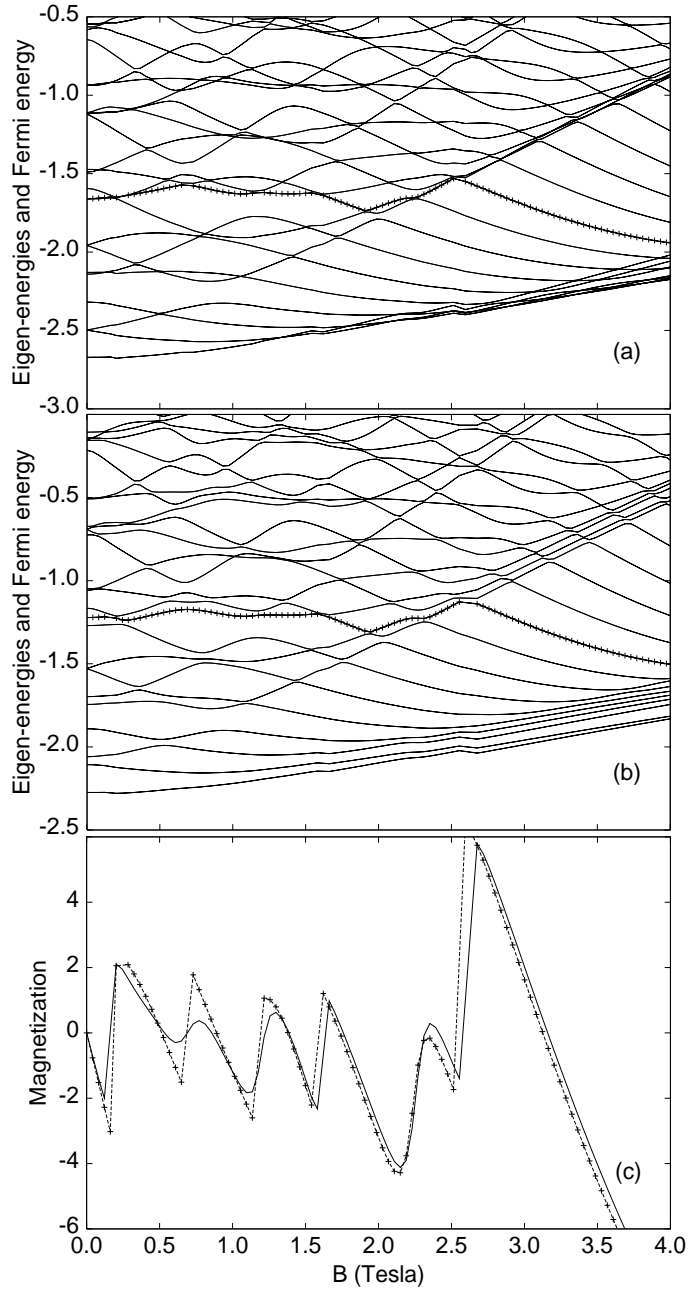


FIG .6. (a) -Energy spectrum , in the Hartree approximation, in the presence of intra-dot electron-electron interaction, but with no inter-dot interaction. The crosses show the Fermi energy. (b) -The same, but with both intra- and inter-dot interaction. The dots are coupled only electrostatically, and the number of electrons is $N_e = 10$ in each dot. (c) -The magnetization for the two cases: for intra-dot interaction only, with the dashed line and crosses, and for the total interaction, with the solid line. The whole system has 20×10 sites, and the interaction parameter is $U_c = 0.4$.

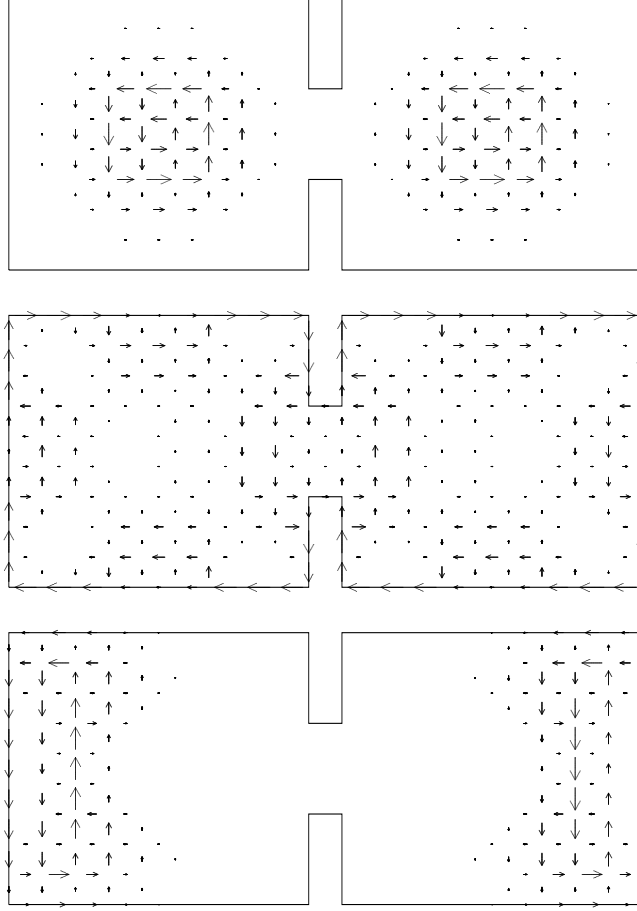


FIG .7. Persistent currents in double dot. Top: The local current corresponding to the eigenstate # 1 at $U_c = 0$. Middle: The same for the eigenstate # 46. Bottom : The local current corresponding to the Hartree eigenstate # 1 at $U_c = 0.4$

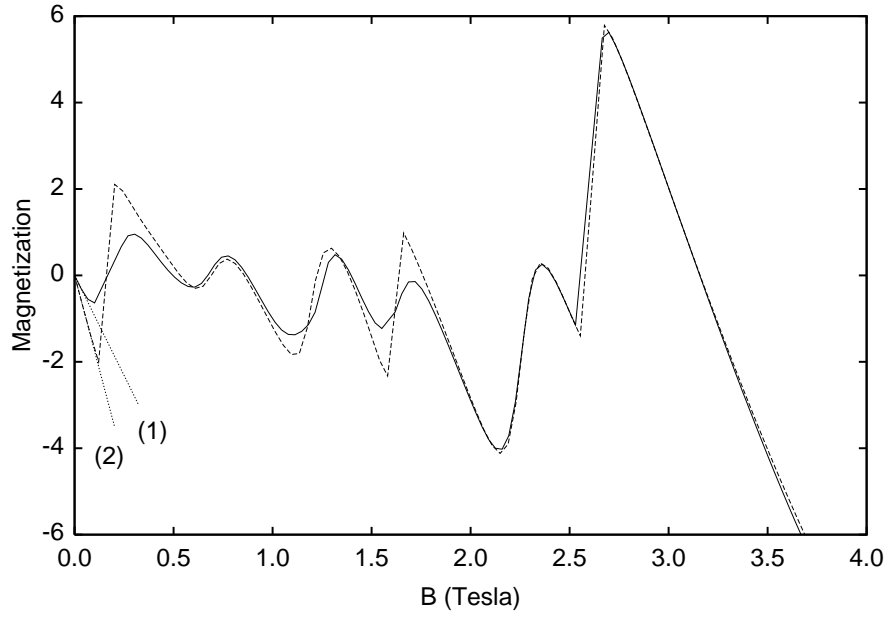


FIG .8. The total magnetization of the double dot in the presence of the electrostatic coupling : with tunnel coupling $t = 0.4t$ (full line) and without tunnel coupling $t = 0$ (dashed). The straight lines (1) and (2) are the tangents at the magnetization curves in the low field domain for the two cases.

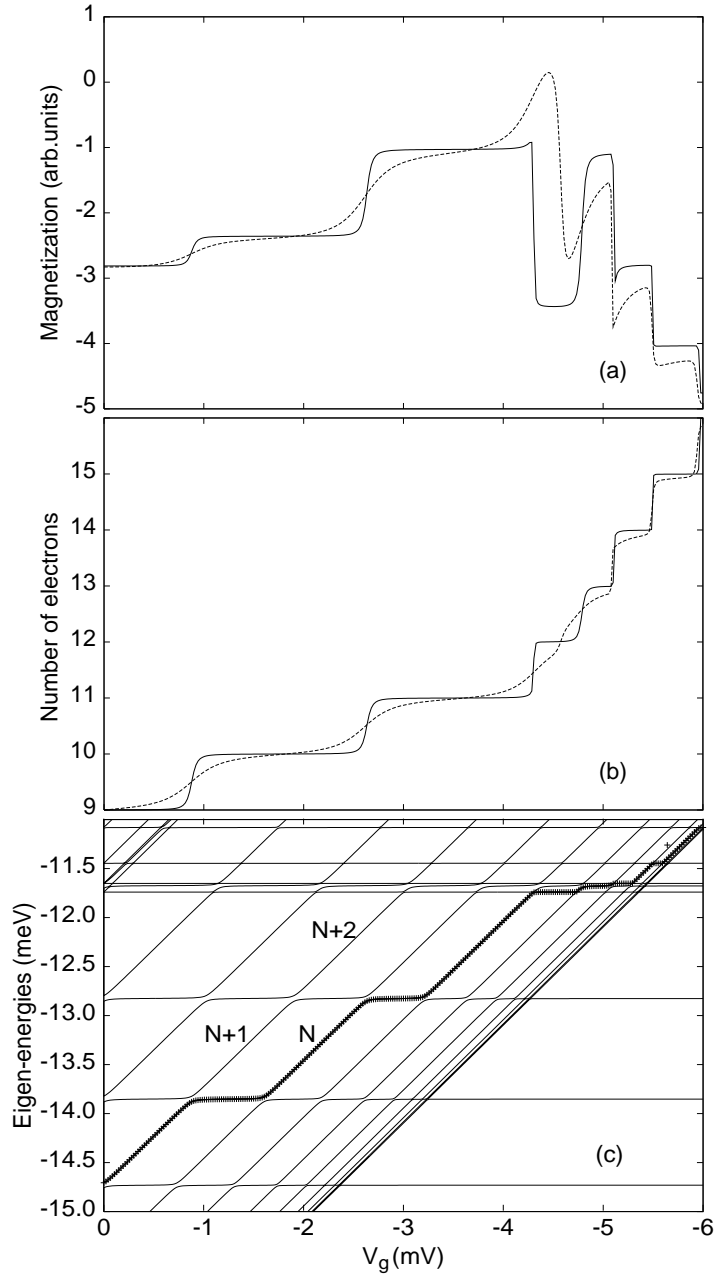


FIG. 9. The magnetization (a), number of electrons in the nondetuned dot 1 (b) and a piece of the energy spectrum (c) versus the gate potential V_g . The following parameters have been used: $\alpha = 0.1$ (corresponding to $B = 4$ T), $\beta = 0.1$ (the full line) and $\beta = 0.4$ (the dashed line). The Fermi level corresponding to $N = 18$ is also shown.

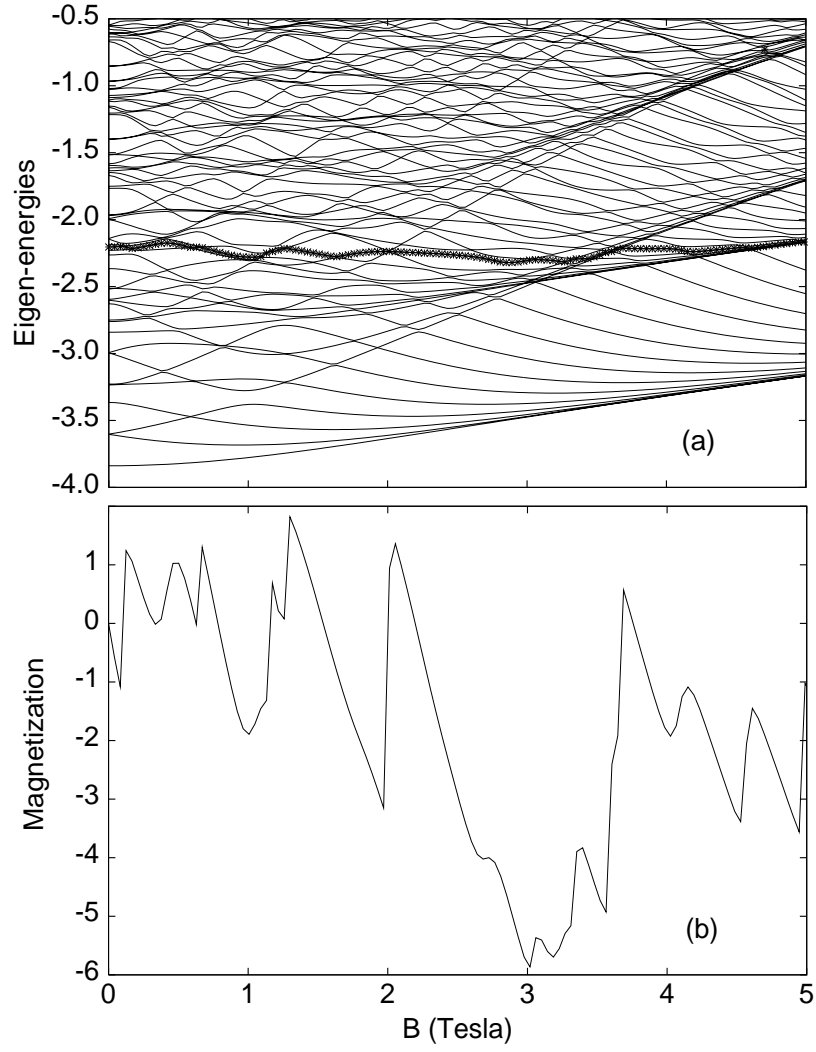


FIG .10. The lower part of the energy spectrum (a) and the ground state magnetization (b) of a detuned double dot at $V_g = 5 \text{ mV}$. The Fermi level corresponds to 20 electrons accommodated in the system. The tunnel coupling is $t = 0.4$.